Journal of Nuclear Materials 390–391 (2009) 315–318

Contents lists available at ScienceDirect

Journal of Nuclear Materials

journal homepage: www.elsevier.com/locate/jnucmat

2D divertor design calculations for the national high-power advanced torus experiment

J.M. Canik [a,*], R. Maingi [a], L. Owen [a], J. Menard [b], R. Goldston [b], M. Kotschenreuther [c], P. Valanju [c], S. Mahajan [c]

[a] Oak Ridge National Laboratory, 1 Bethel Valley Rd., Oak Ridge, TN, USA
[b] Princeton Plasma Physics Laboratory, Princeton, NJ, USA
[c] University of Texas-Austin, Austin, TX, USA

ARTICLE INFO

PACS:
52.55.Fa
52.55.Rk

ABSTRACT

The national high-power advanced torus experiment is a concept for a new facility to address the FESAC theme of 'taming the plasma-material interface'. This concept exploits the compactness and excellent access provided by low aspect ratio to achieve a high ratio of exhaust power to major radius in order to study the integration of high-performance, long-pulse plasmas with a reactor-relevant high heat flux plasma boundary. Predictions of the scrape-off-layer plasma characteristics are presented, as calculated with the 2D edge modeling code SOLPS. Calculations in a variety of magnetic geometries indicate that very high levels of divertor heat flux can be expected, with peak values far in excess of the power handling capabilities of presently-used materials. Possible methods to reduce the heat flux to acceptable levels are discussed.

1. Introduction

A major challenge to the development of an economical fusion power plant is the handling of the large power exhaust. The ratio of exhaust power to major radius, P/R, is often used as a figure of merit for the power load on the divertor. In terms of this parameter, the leap from the current or near-future generation of experiments (including ITER) to a DEMO plant is a factor of ~4 [1]. The National High-power Advanced Torus Experiment (NHTX) concept exploits the compactness of the spherical torus to achieve very high levels of P/R in a compact, cost-effective device with excellent access for diagnostics and change-out of internal components [2]. The mission of NHTX is to study the integration of high-performance plasmas, with good confinement and stability in long-pulse discharges, with a high heat flux plasma boundary. NHTX is presently conceived with major and minor radii of 1.0 and 0.55 m, respectively, and it will operate with plasma current and magnetic field of up to 3.5 MA and 2.0 T, respectively. The total planned auxiliary heating power is 50 MW, with 30 MW from neutral beam injection. This paper presents 2D modeling of the NHTX edge plasma to identify the operational windows of the divertor temperature, density, and heat flux.

2. Modeling assumptions and base magnetic geometries

The scrape-off-layer (SOL) plasma parameters and target heat flux profiles have been calculated using the SOLPS suite of codes [3]. In the fully coupled plasma/neutral modeling presented here, the plasma transport is treated with the fluid code B2.5 [4], and the neutral transport is calculated using the Monte Carlo code EIRENE [5]. In the present work, the 1996 version of EIRENE is used, with hydrogen ionization and recombination rates from [6], and charge exchange and molecular dissociation rates from [7] (elastic collisions of molecules and ions are not included). Transport is classical parallel to the magnetic field, with kinetic limits imposed when transport approaches the free-streaming rates. In the direction normal to the flux surfaces, transport is computed with assumed anomalous transport coefficients; here, spatially uniform coefficients are used, with the particle diffusivity $D = 0.4\ m^2/s$, and thermal diffusivities $\chi_e = \chi_i = 1.6\ m^2/s$. These values, somewhat higher than those typically measured in H-mode plasmas in higher aspect ratio tokamaks [8], are chosen to give SOL widths consistent with ITER projections of 5 mm (see Section 3.1). Classical drifts are not included in these simulations. Pumping is simulated at the divertor targets by specifying a recycling coefficient of $R = 0.95$ (an exception is the case of the vertical target modeling described in Section 4.1); the recycling coefficients at the chamber wall are set to unity. Here $R < 1$ is used to simulate lithiated targets for particle control, and the low value of $R = 0.95$ is used to simulate the strong particle pumping that is expected with lithium targets. The plasma parameters at the inner boundary (typically ~5–10 cm inside the separatrix at the midplane) are inputs: the density at the inner boundary is set to $1.5 \times 10^{20}\ m^{-3}$ (roughly half the Greenwald density at full plasma current). Two input powers are used, 30 and 50 MW, split evenly between the ions and electrons. In most cases, the modeling assumes pure deuterium

* Corresponding author.
E-mail address: canikjm@ornl.gov (J.M. Canik).

0022-3115/$ - see front matter © 2009 Elsevier B.V. All rights reserved.
doi:10.1016/j.jnucmat.2009.01.143

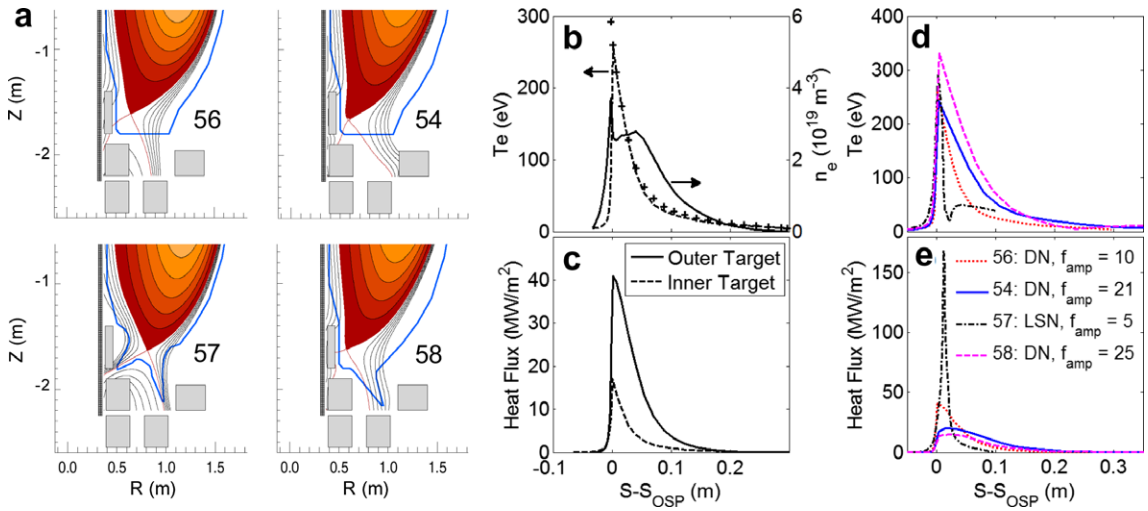

Fig. 1. (a) Base magnetic and target geometries for which calculations are performed. Configuration labels and main characteristics are: 56 – DN, horizontal target, f_{amp} = 10; 54 – DN, horizontal target, f_{amp} = 21; 57 – LSN, slot divertor, f_{amp} = 5; 58 – DN, slot divertor, f_{amp} = 25. Profiles of (b) electron density and temperature and (c) total heat flux at the target plates for configuration 56; upstream temperature is shown as '+' symbols in (b). Profiles of (d) electron temperature and (e) total heat flux at the outer target for all four configurations. The core boundary conditions are density = 1.5×10^{20} m^{-3}, input power = 30 MW.

plasmas, with impurity radiation considered by a constant impurity concentration (again the exception is the vertical target case, where carbon sputtering is included self-consistently).

The four primary magnetic configurations considered are shown in Fig. 1(a). Configurations 56 and 54 are both connected double null (DN) shapes with horizontal divertor targets, differing mainly in the flux expansion near the target. These can be quantified using f_{amp}, which is defined as the distance along the target between the separatrix and a chosen flux surface divided by the separation of the two surfaces at the outer midplane (a midplane separation of 5 mm is used here). This factor accounts for the increase of heat flux width that can be expected due to the combination of flux expansion and poloidal inclination of the target plate. The value of f_{amp} is 21 for configuration 54 and 10 for configuration 56; these can be compared to the ITER value of ~10 [9]. Cases 57 and 58 have more closed slot divertor geometries. Configuration 57 is a lower single null geometry, and has a low value of f_{amp} = 5. Case 58 is a double null with f_{amp} = 25; the high value is due in part to target plate tilting.

3. Modeled divertor parameters in base configurations

3.1. Expected heat fluxes in low flux expansion DN with a horizontal target

The calculated profiles of electron temperature T_e and density n_e along the outer target are shown in Fig. 1(b) for configuration 56, the low flux expansion DN. The input power in this simulation is 30 MW, giving a value of P/R = 30 MW/m, which can be compared to the ITER value of $P/R \sim 16$ MW/m. Pure deuterium plasma is considered. As the figure shows, T_e is over 200 eV near the outer strike point, and remains above 50 eV for ~5 cm along the target. These values are essentially equal to the upstream temperatures, also shown in the figure, and indicate that SOL transport is in the sheath-limited regime [10]. The n_e profile at the target is broader than T_e, and the fairly low value of $\sim 3 \times 10^{19}$ m^{-3} is also similar to the upstream parameters, reflecting the sheath-limited transport. In the simulation, 25 MW goes to the outer SOL, and 5 MW to the inner. The heat flows in each SOL are split evenly between the upper and lower targets, and less than 20 kW crosses the outermost grid edge. The heat flux profile (Fig. 1(c)) shows a decay length of ~5 cm at the outer target, or ~5 mm mapped to the midplane; this is similar to the projected value for ITER [11]. This profile represents the power flux carried by the plasma ions and electrons as well as recombination on the targets; radiated power is not included since, as shown below, this is small in these simulations. The peak heat flux at the outer target is 40 MW/m^2, well above the material limit of 10 MW/m^2 used in the ITER design [9]. The heat flux at the inner target has a peak value of ~15 MW/m^2. Since this is closer to the accepted limits, the parameters at the outer target are the focus of the present work.

The low divertor density is due partially to the strong pumping used in the modeling; calculations assuming a higher recycling coefficient of R = 0.99 show that the density ~5–10 cm away from the strike point is increased to more than $\sim 3 \times 10^{20}$ m^{-3}. However, these simulations show that near the strike point, transport remains sheath-limited, and the temperature, density and heat flux are essentially the same as the low recycling case. Hence, the divertor plasma parameters in the region in which the peak heat flux is expected are not sensitive to the recycling conditions assumed.

Impurity radiation has been considered by assuming a fixed impurity concentration f_{imp}, and adding a radiated power density based on $P = n_e n_{imp} L(T_e) = f_{imp} n_e^2 L(T_e)$, where $L(T_e)$ is the radiation power function [12]. Three impurity species have been considered: carbon, neon, and argon. For each of these, radiation has been added to the model using a concentration of 4% in the SOL. In the case of both carbon and neon, the total additional impurity radiation is only ~1 MW. This is due to the low density and high temperature of the divertor plasmas associated with the sheath-limited regime; the radiation function drops sharply for temperatures above 10 eV for the case of carbon, and 30 eV for neon. As a result, radiation is not an efficient heat sink using these species. Even though argon radiates more strongly at higher temperatures, 4% only adds 4 MW to the radiated power. Clearly this is small compared to the input power of 30 MW, and only reduces the peak heat flux to 37 MW/m^2. Note that the radiation model used here assumes a coronal equilibrium. While transport effects can increase impurity radiation at high temperatures [10], due to the low divertor plasma density in the cases shown here the total radiation including these effects is expected to remain small. This has been confirmed by calculations in which the radiation function used in the SOL has a constant value equal to the maximum of the coronal rate. In this case, a 4% carbon concentration yields total

radiation that remains less than 10% of the input power. More realistic impurity modeling including transport is described in Section 4.1.

3.2. Heat flux variation with geometry

Calculations have been performed for the four configurations shown in Fig. 1(a), using an input power of 30 MW and assuming pure deuterium plasmas in all cases. The calculated divertor T_e are shown in Fig. 1(d), and the heat flux at the outer divertor in Fig. 1(e). Similar to the case shown previously, T_e near the strike point are all above 200 eV. This indicates that, in all geometries considered, the SOL is in the sheath-limited regime – at least near the separatrix, where the highest values of the heat flux can be expected. Impurity radiation can thus be expected to be inefficient in these cases. The heat flux, however, shows a strong dependence on the magnetic geometry. The lower single null case has the lowest flux expansion; this configuration gives a peak flux of 150 MW/m^2. In this deep slot geometry, the local value of f_{amp} shows a strong variation along the target which is not captured by the value taken at the flux surface 5 mm outside the separatrix as described above; at the location of peak heat flux, the local f_{amp} is ~2.5, leading to the very high peak heat flux. The high flux expansion DN cases, 54 and 58, show the lowest peak heat fluxes, with values of 20 and 16 MW/m^2, respectively. These results illustrate the strong effect of the number of nulls and the target flux expansion on heat flux profiles. Using this control, the heat flux values can be *chosen* to either be minimized for power handling purposes, or maximized in order to test PFCs at high power densities. However, it should be noted that even at this power level, which is 60% of the full planned heating power for NHTX, the peak fluxes in all four configurations are in excess of 10 MW/m^2, illustrating the challenge of power handling at high P/R.

4. Possible solutions

4.1. Vertical target

To explore possible methods for lowering the peak heat flux to values below 10 MW/m^2, a vertical target configuration has been modeled. The principle of this design is to tilt the plate to increases the plasma-wetted area, with the orientation such that the recycled neutrals are directed towards the separatrix strike point [13]. This raises n_e near the strike point and promotes partial detachment, the operational scenario for the ITER divertor [14]. The magnetic equilibrium used for the vertical target calculation is 54 (high flux expansion DN). The divertor targets are similar to those shown in Fig. 1(a) for case 58, with the plate adjusted so that the angle of incidence between the magnetic field lines and the plate is about 1° across the target. The sheath boundary conditions applied in this case are unchanged from those used in the simulations described in Section 3, although it should be noted that these may not be correct for the very low angle of incidence of these inclined targets [10]. The recycling coefficient at the target is set to unity; pumping is performed in the private flux region, where the recycling coefficient at the wall segment indicated in Fig. 2(a) is set to $R = 0.95$. Carbon is sputtered from the targets using a constant chemical sputtering yield of 1%. Additional deuterium gas is puffed into the divertor in the private flux region, as shown in Fig. 2(a).

In order to test the power handling capability of this geometry, 50 MW is used as the input power of the simulation. The calculated outer divertor profiles of n_e and T_e are shown in Fig. 2(b) for a case with gas puff rate $\Gamma^{puff} = 10^{23}$/s; the magnitude of the gas puff can be compared to the total target ion flux of ~8×10^{23}/s. Under these

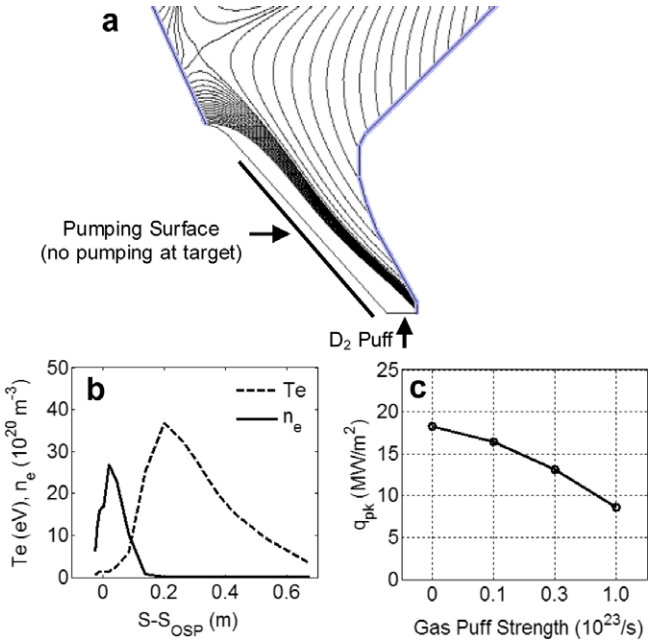

Fig. 2. Vertical target (a) geometry, (b) profiles of electron density and temperature at the outer target plate, and (c) peak heat flux versus the strength of gas puff into the divertor. The core density is 1.5×10^{20} m^{-3}, the input power is 50 MW.

conditions partial detachment can be achieved at the strike point, with $T_e \sim 1$ eV. The high n_e and low T_e in this regime allows higher radiated power; the case shown has ~14 MW of carbon radiation (Z_{eff} at the inner boundary in this case is 1.5). Fig. 2(c) shows that the peak heat flux can be reduced to below 10 MW/m^2 at high values of Γ^{puff}. The decrease of the peak heat flux is primarily due to increasing carbon radiation as the gas puff is increased, with an additional reduction due to a broadening of the heat flux profiles. Note that the highest Γ^{puff} shown is approximately equal to the ITER limit for DT gas throughput due to tritium inventory considerations [15]. The solution is admittedly rather tenuous: when P_{in} is raised to 60 MW, the peak heat flux increases to 13 MW/m^2 at $\Gamma^{puff} = 10^{23}$/s. Although this is more heating power than anticipated, the same effect can be achieved by unbalancing the double null; by using a single null configuration, NHTX could test this solution at approximately twice the power to the divertor as the case shown here.

4.2. Super-X divertor

The second possible method to lower the heat flux described below is a Super-X Divertor [16] configuration. The strategy here is to bring the outer target plates to larger major radius (in the present case 2.2 m), both decreasing the effective P/R and increasing the connection lengths. The Super-X configuration is shown in Fig. 3(a); the flux expansion near the X-point is similar to configuration 54. The connection length measured 5 mm outside the separatrix at the outer midplane is increased from ~10 m in configuration 54 to ~40 m in the Super-X configuration. The Super-X magnetic field does not require any alterations to the toroidal field coil set, which is the same as in the standard divertor configurations. Two additional poloidal field coils are used in the Super-X case shown here; however the total current in the poloidal field coils is changed by less than ~5% compared to the standard divertor. The modeling was performed as in Section 2: pure deuterium plasmas with target plate pumping. The results of a n_e scan are shown in Fig. 3(b); the inner boundary densities used in these cases are 0.75, 1.5, and 3.0×10^{20} m^{-3}, and the input power is

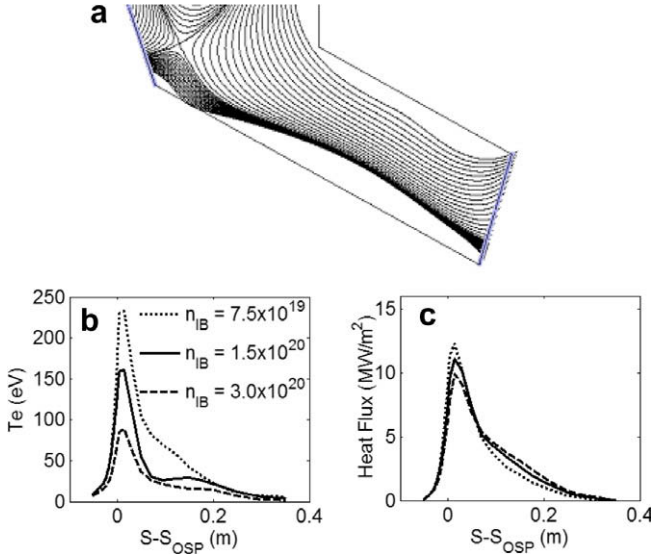

Fig. 3. Super-X Divertor (a) geometry (major radius of the outer strike point is 2.2 m), and profiles of (b) electron temperature and (c) heat flux at the outer target. Inner boundary density is 0.75–3.0 $\times$ 10^{20} m^{-3}, input power is 50 MW.

50 MW. With an inner boundary density of 1.5 $\times$ 10^{20}, the peak temperature is ~150 eV. Although this is less than the values with standard divertors (c.f. Fig. 1(d)), the transport remains in the sheath-limited regime. The peak heat fluxes, (Fig. 3(c)), are in the range of 10–12 MW/m^2. This is much lower than the values shown in Section 2 (in which a lower input power of 30 MW was used), and is approaching manageable levels with conventional technologies. Further optimization could be made as in the vertical target case; indeed this would be necessary in order to reduce the plasma temperature at the target so that high physical sputtering rates can be avoided. Nonetheless, the results shown here indicate the potential of the Super-X concept for allowing operation even in the sheath-limited regime, i.e. without requiring high edge densities or partial divertor detachment.

5. Conclusions

The modeling presented shows that NHTX is capable of the design goal of providing a high heat flux edge, with heat fluxes exceeding 100 MW/m^2 in the most extreme case. The magnetic flexibility allows a large variation in the values of the peak heat flux for testing of plasma facing components. For the most part, plasma transport at the expected power levels is sheath-limited, limiting the efficiency of divertor radiation. Two possible solutions have been tested. A conventional vertical target may be capable of handling the heat flux; however, this requires a large gas puff into the divertor and may restrict the equilibrium to a connected double null in order to ensure partial detachment and high radiated power levels. A Super-X divertor has also been modeled, showing that peak heat flux can be reduced nearly to 10 MW/m^2, even in the sheath-limited regime.

Acknowledgements

Research performed by the first author as a Eugene P. Wigner Fellow and staff member at the Oak Ridge National Laboratory, managed by UT-Battelle, LLC, for the US Department of Energy under Contract DE-AC05-00OR22725. Research also supported under contract DE-AC02-76CH03073.

References

[1] J. Menard et al., Physics Design of the National High-Power Advanced Torus Experiment, PPPL Report No. 4252, July 2007.
[2] C. Neumeyer et al., in: Proceedings of the 22nd IEEE/NPSS Symposium on Fusion Engineering, Albuquerque, New Mexico, 17–22 June 2007, p. 1.
[3] R. Schneider et al., Contribution Plasma Phys. 46 (2006) 3.
[4] B. Braams et al., Contribution Plasma Phys. 36 (1996) 276.
[5] D. Reiter et al., Fus. Sci. Technol. 47 (2005) 172. and <http://www.eirene.de>.
[6] K. Sawada, T. Fujimoto, J. Appl. Phys. 78 (1995) 2913.
[7] R.K. Janev et al., Elementary Processes in Hydrogen–Helium Plasmas, Springer-Verlag, Berlin, 1987.
[8] A. Loarte et al., J. Nucl. Mater. 266–269 (1999) 1123.
[9] Progress in the ITER physics basis, Nucl. Fusion 47 (2007) S203 (Chapter 4).
[10] P.C. Stangeby, The Plasma Boundary of Magnetic Fusion Devices, Plasma Physics Series, IoP Publishing Ltd., Bristol, UK, 2000.
[11] A. Kukushkin et al., Nucl. Fus. 43 (2003) 716.
[12] D.E. Post, J. Nucl. Mater. 220–222 (1995) 143.
[13] B. Lipshultz et al., in: Fusion Energy 1996, Proceedings of the 16th International Conference Montreal, 1996, vol. 1, IAEA, Vienna, 1997, p. 425.
[14] A. Kukushkin, H.D. Pacher, Plasma Phys. Control. Fus. 44 (2002) 932.
[15] A.S. Kukushkin et al., J. Nucl. Mater. 290–293 (2001) 887.
[16] M. Kotschenreuther, P.Valanju, S. Mahajan, in: Proceedings of the 49th Meeting of APS Division of Plasma Physics, Orlando, 2007, Bulletin of the American Physical Society, vol. 52, 2007, p. 125.;
P. Valanju et al., in: Presented at the PFC Group Annual Meeting, Albuquerque, NM, 21–23 July 2008.